ICAS-98-7,8,1

A98-31715

From the Hale Gnopter to the Ornithopter- Or How to Take Advantage of Aircraft Flexibility

Céline Pendariès[†‡]

[†] *ONERA-CERT/DCSD, System Control and Flight Dynamics, B.P. 4025, F - 31055 Toulouse Cedex, France*
[‡] *SUPAERO, B.P. 4032, F - 31055 Toulouse Cedex, France*

email: pendaries@cert.fr

Abstract

In order to achieve their outstanding performances, the hale gnopters need a specific design: high aspect-ratio wings and low wing loading. These characteristics imply flexibility, low frequency modes and aeroelastic phenomena at low speed. Therefore, wing flexibility has to be taken into account at the early stage of conceptual aircraft design.
The flight dynamics equations of a free flexible aircraft are presented in this paper. The new aspects of the modelization lies in the full coupling between rigid-body modes and flexible modes.
The first results of this modelization revealed different kinds of instabilities: the classical flutter due to a coupling between flexible modes, and other instabilities due to the coupling between rigid modes and flexible modes, like the instability of the first bending mode, leading to a kind of flapping movement. The evolution of the rigid-body modes with the speed is also clearly affected by the presence of flexible modes.
The propulsion by wing flapping without articulations at the wing-root is then studied to show that this propulsion mode could be an alternative to propellers.

1. Introduction

So as to fly for a very long time or at high altitude, hale gnopters * are characterized by high aspect-ratio wings, low wing loading and thus very flexible structures. The frequencies of flexible modes are very low, around 0.3-0.6 Hz, and get close to the rigid-body modes frequencies. A coupling between rigid and flexible movements usually appears for this type of aircraft. Therefore, the rigid dynamics can no more be analyzed separately from the flexible analysis. Moreover, because of the oustanding performances of these airplanes, the hale design is very sensitive to the optimization process, developped in the first phase of aircraft design. It is thus necessary to shift the flexibility analysis from the preliminary to the conceptual design process, so as to guarantee a stable aircraft. We need methods that are well adapted to aircraft design, that is to say, simple, rapid, but whose limits are known.

In a former article,[(1)] a modelisation of the embedded wing, dubbed *Flutty*, based on the finite element method with few beam elements had been presented. This model had been numerically and experimentally validated.[(1)]From *Flutty*, the flight dynamics equations of the entire free aircraft had been derived, leading to a software *Super Flutty*, the object of this paper. *Super Flutty* always fits well with the preliminary design because the structural modelisation is simple: beam elements, simplified profile. It is computationally efficient so as to be integrated in an optimisation process. The first results, obtained with *Super Flutty*, show obviously the influence of rigid-body modes on the flexible modes and the other way round, and demonstrate the necessity of introducing flexibility analysis very early in the design process.

A new concept of ornithopter [†] had been introduced also in[(1)] as a pedagogic application of flexibility. It could be an alternative to propulsion by propellers. Indeed, the higher you fly, the larger your propeller is. The idea was to use the natural wing flexibility by exciting the first bending mode in a flapping movement to produce thrust. Efficiency and powers were computed with *Flutty* on an embedded wing and showed that flapping without articulations at the wing root gave sufficient thrust for cruise flight with an efficiency equivalent to a propeller. These works are now extended to the free wing.

---

* *HALE* is an acronym for High Altitude Long Endurance
The term *gnopter* denotes an unmanned aircraft, often named UAV (Uninhabited Aerial Vehicle)

[†] *Ornithopter* designates an aircraft with flapping wing

21st ICAS Congress
13-18 September 1998
Melbourne, Australia

Notations

F_N or N	Reference frame (derivation)
F_A or A	Aerodynamic frame
F_B or B	Body frame (projection)
O_N	Reference frame origin
G_0	Body frame origin
ac	Aerodynamic center
c	aerodynamic chord
${}^N\omega^B$	Rotation of frame F_B relative to frame F_N
$\frac{{}^D d}{dt} H$	Derivative of H with respect to the frame D
R^{PQ}	Vector $\vec{PQ}$
U, V, W	Absolute speed of G_0 projected in body frame
u, v, w	Displacement of the center of mass of a section (body or wing) along X_b, Y_b, Z_b respectively
θ_x, θ_y, θ_z	Deformation angles (body or wing)
N_u, N_v, N_w, N_{θ_y}	Interpolation polynom of structural displacements
χ	Whole degrees of freedom vector
χ_o	Degrees of freedom of G_0
χ_s	Structural degrees of freedom
$\underline{N_u}$	$\int \rho S \, N_u dl$ Integration on the aircraft of the interpolation function multiplied by the lineic mass (cf 2.4)
$\underline{u}$	$\int \rho S \, N_u dl \chi_s$

2. Flight Dynamics of Free Flexible Aircraft

2.1 Introduction

This section deals with the modelization of the flight dynamics of a free flexible aircraft. The energetic approach had been chosen against the conventional approach, because it is more appropriate to the finite element method.

To position the problem, the choice of the relative frame will be detailed. The different parts of the Lagrange's Equations will be written, and particularly the kinetic energy, which is very interesting in order to analyze the coupling between rigid and flexible. Then, the aerodynamic forces will be introduced in the equations.

The structural modelization of the body and the wing will not be detailed, the reader can report himself to the previous article.[1]

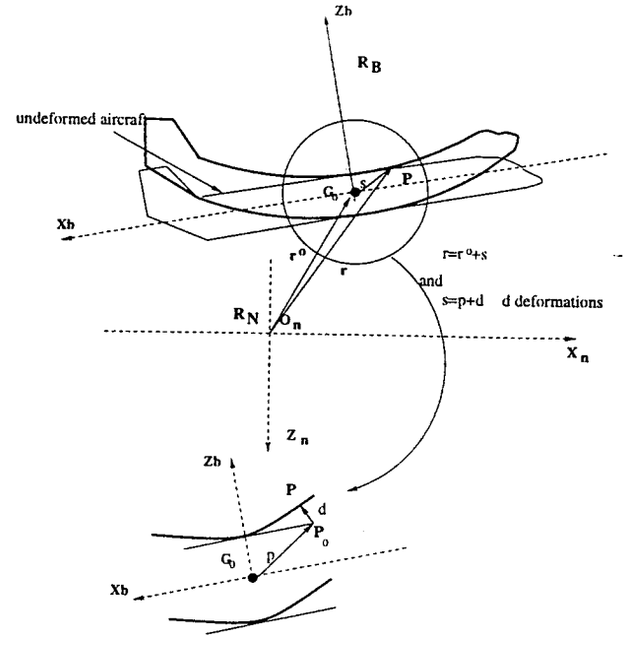

Fig. 1. Body frame definition

2.2 Relative Frame Choice

As written above, the choice of the relative frame is very important because it conditions the complexity of the equations but also their physical signification. This is the frame in which the flight dynamics equations will be written, and the aerodynamic forces projected.

In our approach, the physical meaning will be favoured against the equations simplicity, which makes the originality of our approach. The notion of "mean reference frame" or "mean axes", usually used to define the body frame, will not be treated. Then, no assumptions will be made neither on the axes nor on the position of the instantaneous center of gravity. In[2,3] the authors choose the mean axes whose properties contribute to simplifying the kinetic energy expression. These properties do not appear obvious to me, as the system is under aerodynamic loads. Therefore, we have defined our own relative frame.

The origin G_0 of the body frame F_B is defined as the center of mass of the undeformed aircraft, it is a real geometrical point. And the axes associated to this point are the eigen axes of the body section, whose center of mass is G_0. X_b is the axis orthogonal to the section toward the rear of the aircraft, Y_b and Z_b are the elastic axes associated to the section (cf Fig. 1, page 2).

Let us now define the displacements of every point of the aircraft regard to the Earth reference frame. The position of G_0 is then completely defined by the projection of $R^{O_N G_0}$ in the body frame. The orientation of the body axes is also referenced by angles. x_0, y_0, z_0 are G_0 coordinates along X_b, Y_b and Z_b respectively, and ϕ_0 is the bank angle between Y_n

Rendaus

and Y_b, ψ_0 the azimuth angle between Z_n and Z_b, and θ_0 the pitch angle between X_n and X_b.

The structural degrees of freedom are noted χ_s; they let us define the node displacements of the wing and the body. The structural nodes are the center of mass of each section considered. χ groups the coordinates of G_0 χ_o, and the structural displacements χ_s.

The vector $s(x,y,z,t) = \boldsymbol{R}^{G_0P}$ where P is a current point of the aircraft, is defined by (cf Fig. 1, page 2):

$$s(x,y,z,t) = \boldsymbol{R}^{G_0P} = \boldsymbol{R}^{G_0P_o} + \boldsymbol{R}^{P_oP} = \boldsymbol{p} + \boldsymbol{d}$$

with $\boldsymbol{p}$, point of the undeformed aircraft and $\boldsymbol{d}$, the deformation (cf Fig. 1, page 2). Body and wing are modelized by the finite element method and the deformation $\boldsymbol{d}$ may be expressed as function of χ_s.

Now, we have expressed the whole displacement of a current point P in the body frame. We will then write the Lagrange's equations of a flexible aircraft, the kinetic energy, the aerodynamic forces and the elastic energy.

2.3 Lagrange's Equations

The Lagrange's equations for the whole aircraft have the following expression:

$$\frac{d}{dt}\frac{\partial L}{\partial \dot{\chi}} - \frac{\partial L}{\partial \chi} + \frac{\partial D}{\partial \dot{\chi}} = Q \qquad (1)$$

where L is the Lagrangian, that is to say the difference in kinetic and potential energy ($L = \mathcal{T} - \mathcal{U}_d - \mathcal{U}_g$), where $\mathcal{T}$ is the kinetic energy, $\mathcal{U}_d$ is the energy of deformation, $\mathcal{U}_g$ the potential energy of gravity, $Q = \frac{\partial \mathcal{W}}{\partial \chi}$ the generalized forces (aerodynamic and propulsion) and D expressing the damping. Since no structural damping will be considered here, (Eq. 1) becomes:

$$\frac{\partial}{\partial t}\left(\frac{\partial(\mathcal{T} - \mathcal{U}_d - \mathcal{U}_g)}{\partial \dot{\chi}}\right) - \frac{\partial(\mathcal{T} - \mathcal{U}_d - \mathcal{U}_g)}{\partial \chi} = \frac{\partial \mathcal{W}}{\partial \chi} \qquad (2)$$

For equations simplification, we will define new angles ϕ_b, θ_b and ψ_b as follows

$$p = \dot{\phi}_b = \dot{\phi}_0 - \dot{\psi}_0 \sin\theta_0 \qquad (3)$$

$$q = \dot{\psi}_b = \dot{\psi}_0 \cos\theta_0 \sin\phi_0 + \dot{\theta}_0 \cos\phi_0 \qquad (4)$$

$$r = \dot{\theta}_b = \dot{\psi}_0 \cos\theta_0 \cos\phi_0 - \dot{\theta}_0 \sin\phi_0 \qquad (5)$$

For purpose of clarity and conciseness, the only terms concerning x_0, ϕ_b and χ_s will be presented, when developped. At the time of the complete writing of the Lagrange's equations, we have noticed, as we will see later (cf 2.7) , that it was more comfortable to consider than

$$\frac{\partial}{\partial t}\left(\frac{\partial L}{\partial \dot{\phi_b}}\right) - \frac{\partial L}{\partial \phi_b} - y_0 \frac{\partial \dot{\mathcal{W}}}{\partial z_0} + z_0 \frac{\partial \mathcal{W}}{\partial y_0}$$

$$\frac{\partial}{\partial t}\left(\frac{\partial L}{\partial \dot{\phi_b}}\right) - \frac{\partial L}{\partial \phi_b}$$

All these preceeding terms will be now detailed.

2.4 Kinetic Energy

The kinetic energy is expressed by writing the velocity of each point of the aircraft, which is the derivative of $\boldsymbol{R}^{O_NP}$ with respect to the reference frame F_N.

$$\boldsymbol{R}^{O_NP} = \boldsymbol{R}^{O_NG_0} + \boldsymbol{R}^{G_0P}$$

and

$$\frac{^Nd}{dt}\boldsymbol{R}^{O_NP} = \frac{^Nd}{dt}\boldsymbol{R}^{O_NG_0} + \frac{^Bd}{dt}\boldsymbol{R}^{G_0P} + {}^N\boldsymbol{\omega}^B \wedge \boldsymbol{R}^{G_0P}$$

and

$$2\mathcal{T} = \int_V \rho \left(\frac{^Nd}{dt}\boldsymbol{R}^{O_NP}\right) \cdot \left(\frac{^Nd}{dt}\boldsymbol{R}^{O_NP}\right) dv$$

The kinetic energy will be then subdivided in six terms, each term having a special signification.

$$2\mathcal{T} = 2\mathcal{T}_1 + 2\mathcal{T}_2 + 2\mathcal{T}_3 + 2\mathcal{T}_4 + 2\mathcal{T}_5 + 2\mathcal{T}_6 \qquad (6)$$

The first term $2\mathcal{T}_1$ concerns the energy due to the rigid movement:

$$2\mathcal{T}_1 = \left(\frac{^Nd}{dt}\boldsymbol{R}^{O_NG_0}\right) \cdot \left(\frac{^Nd}{dt}\boldsymbol{R}^{O_NG_0}\right) \int_V \rho dv \qquad (7)$$

The second term is the energy only due to the deformations

$$2\mathcal{T}_2 = \int_V \rho \left(\frac{^Bd}{dt}\boldsymbol{R}^{G_0P} \cdot \frac{^Bd}{dt}\boldsymbol{R}^{G_0P}\right) dv \qquad (8)$$

and the following terms relate to the coupling between rigid and flexible movements.

$$2\mathcal{T}_3 = 2\left(\frac{^Nd}{dt}\boldsymbol{R}^{O_NG_0}\right) \int_V \rho \frac{^Bd}{dt}\boldsymbol{R}^{G_0P} dv \qquad (9)$$

$$2\mathcal{T}_4 = 2\left(\frac{^Nd}{dt}\boldsymbol{R}^{O_NG_0}\right) \int_V \rho \left({}^N\boldsymbol{\omega}^B \wedge \boldsymbol{R}^{G_0P}\right) dv \qquad (10)$$

$$2\mathcal{T}_5 = \int_V \rho \left(\frac{^Bd}{dt}\boldsymbol{R}^{G_0P}\right) \cdot \left({}^N\boldsymbol{\omega}^B \wedge \boldsymbol{R}^{G_0P}\right) dv \qquad (11)$$

Pendaries

$$2\mathcal{T}_6 = \int_V \rho \left({}^N\boldsymbol{\omega}^B \wedge \boldsymbol{R}^{G_0P} \right) \cdot \left({}^N\boldsymbol{\omega}^B \wedge \boldsymbol{R}^{G_0P} \right) d\mathcal{V} \quad (12)$$

The rotation of the body frame relative to the reference frame can be expressed as ${}^N\boldsymbol{\omega}^{BT} = [p\ q\ r]$, with the classical angular velocities, p the roll rate, q the pitch rate and r the yaw rate, projected in F_B.

Each kinetic term has a special signification in the coupling between rigid and flexible behaviours. As an example, the third term represents the coupling between the rigid displacements and the flexible ones; with the notations,

$$\frac{\partial}{\partial t}\left(\frac{\partial \mathcal{T}_3}{\partial \dot{\chi}_s}\right) - \frac{\partial \mathcal{T}_3}{\partial \chi_s} = \dot{U}\underline{N_u}^T + \dot{V}\underline{N_v}^T + \dot{W}\underline{N_w}^T$$

Only the two first terms and the last one of kinetic energy will be developped.

First Term Let us note the mass of the whole aircraft M_t and project $\frac{{}^N d}{dt}\boldsymbol{R}^{O_N G_0}$ in the body frame F_B

$$\frac{{}^N d}{dt}\boldsymbol{R}^{O_N G_0} = U\boldsymbol{i} + V\boldsymbol{j} + W\boldsymbol{k}$$

then

$$2\mathcal{T}_1 = M_t \left(U^2 + V^2 + W^2\right) \quad (13)$$

and

$$\frac{{}^N d}{dt}\boldsymbol{R}^{O_N G_0} = \frac{{}^B d}{dt}\boldsymbol{R}^{O_N G_0} + {}^N\boldsymbol{\omega}^B \wedge \boldsymbol{R}^{O_N G_0} \quad (14)$$

With these last remarks, the first term of Lagrange's equations may be written as

$$\frac{\partial}{\partial t}\left(\frac{\partial \mathcal{T}_1}{\partial \dot{x}_0}\right) - \frac{\partial \mathcal{T}_1}{\partial x_0} = M_t \left(\dot{U} - rV + qW\right) \quad (15)$$

$$\frac{\partial}{\partial t}\left(\frac{\partial \mathcal{T}_1}{\partial \dot{\phi}_b}\right) - \frac{\partial \mathcal{T}_1}{\partial \phi_b} - y_0\frac{\partial \mathcal{W}}{\partial z_0} + z_0\frac{\partial \mathcal{W}}{\partial y_0} = 0 \quad (16)$$

$$\frac{\partial}{\partial t}\left(\frac{\partial \mathcal{T}_1}{\partial \dot{\chi}_s}\right) - \frac{\partial \mathcal{T}_1}{\partial \chi_s} = 0 \quad (17)$$

This first term is present in the flight dynamics equations of a rigid aircraft.

Second term This terms corresponds to the kinetic energy due to the structural deformations and if the movements of our elastic system are small enough, the kinetic energy $\mathcal{T}$ may be written in a quadratic form (Eq. 18)

$$\mathcal{T} = \frac{1}{2}\dot{\boldsymbol{\chi}}_s{}^T [\mathcal{M}]\, \dot{\boldsymbol{\chi}}_s \quad (18)$$

where $[\mathcal{M}]$ is the structural mass matrix, calculated with the finite element method.

Then, the Lagrange's term may be written as follows:

$$\frac{\partial}{\partial t}\left(\frac{\partial \mathcal{T}_2}{\partial \dot{\chi}_s}\right) - \frac{\partial \mathcal{T}_2}{\partial \chi_s} = [\mathcal{M}]\, \ddot{\boldsymbol{\chi}}_s \quad (19)$$

the others lines of Lagrange's equations are obviously equal to zero.

Sixth term The sixth kinetic energy term for an elementary volume $d\mathcal{V}$ is

$$2d\mathcal{T}_6 = \rho \left[(qw - rv)^2 + (ru - pw)^2 + (pv - qu)^2 \right] d\mathcal{V}$$

Then obviously,

$$\frac{\partial}{\partial t}\left(\frac{\partial \mathcal{T}_6}{\partial \dot{x}_0}\right) - \frac{\partial \mathcal{T}_6}{\partial x_0} = 0$$

and the term derivated with respect to ϕ_b may be subdivided in three terms;

$$\frac{\partial}{\partial t}\left(\frac{\partial \mathcal{T}_6}{\partial \dot{\phi}_b}\right) - \frac{\partial \mathcal{T}_6}{\partial \phi_b} = Q_1 + Q_2 + Q_3$$

the first one is the rigid contribution that we have in the flight dynamics equations of a rigid aircraft,

$$\begin{aligned} Q_1 = {} & \mathcal{J}_{xx}\dot{p} - \left(\mathcal{J}_{xy}\dot{q} + \mathcal{J}_{xz}\dot{r}\right) \\ & + \left(\mathcal{J}_{zz} - \mathcal{J}_{yy}\right) qr + \left(\mathcal{J}_{xy}r - \mathcal{J}_{xz}q\right) p \\ & + \left(r^2 - q^2\right) \mathcal{J}_{yz} \end{aligned}$$

the other terms will not be detailled here, but the second term reflects the inertia variations due to the structural deformations and the third one points up the evolution of inertia with time.

The previous expressions show the importance of the choice of body frame, though the different terms of kinetic energy, pointing up the coupling between rigid and flexible motions.

2.5 Elastic Energy $\mathcal{U}_d$

With the assumptions of small deformations, the elastic energy $\mathcal{U}_d$ may be written under a quadratic form (Eq. 20)

$$\mathcal{U}_d = \frac{1}{2}\boldsymbol{\chi}_s{}^T [\mathcal{K}]\, \boldsymbol{\chi}_s \quad (20)$$

where $[\mathcal{K}]$ is the structural stiffness matrix, calculated with the finite element method.

Then the Lagrange's term, concerning the elastic energy becomes

$$-\frac{\partial}{\partial t}\left(\frac{\partial \mathcal{U}_d}{\partial \dot{\chi}_s}\right) + \frac{\partial (\mathcal{U}_d)}{\partial \chi_s} = [\mathcal{K}]\, \chi_s \quad (21)$$

Pendaries

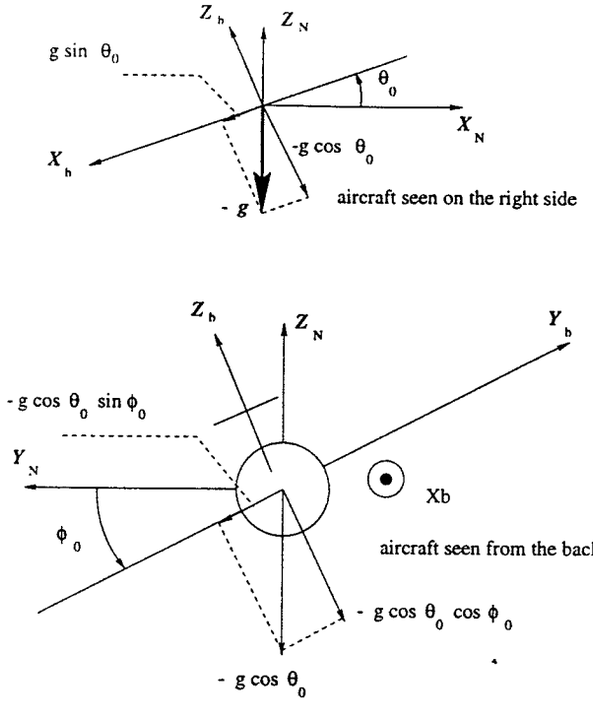

Fig. 2. Work of gravity force

The lines of the Lagrange's equations concerning the rigid movement are obviously equal to zero.

2.6 Gravity Potential Energy $\mathcal{U}_g$

In this section, the work of the weight acting on the flexible aircraft will be presented. Axes orientation and convention are described on Fig. 2, page 5. In projection in the body frame, g will have the following components:

$$\mathrm{g}^T = \{g\sin\theta_0,\ -g\cos\theta_0\sin\phi_0,\ -g\cos\theta_0\cos\phi_0\} \quad (22)$$

The gravity potential energy is written:

$$\mathcal{U}_g = \int_V \rho \mathbf{g}\cdot\boldsymbol{r}\,dv \quad (23)$$

with $r = \begin{Bmatrix} x_0 + u(x,y,z,t) \\ y_0 + v(x,y,z,t) \\ z_0 + w(x,y,z,t) \end{Bmatrix}$

The term $\frac{\partial}{\partial t}\left(\frac{\partial \mathcal{U}_g}{\partial \dot{\chi}}\right)$ is null.

$$\frac{\partial \mathcal{U}_g}{\partial x_0} = M_t g \sin\theta_0$$

$$\frac{\partial \mathcal{U}_g}{\partial \phi_b} - y_0\frac{\partial \mathcal{U}_g}{\partial z_0} + z_0\frac{\partial \mathcal{U}_g}{\partial y_0} = g\cos\theta_0\left[-\cos\phi_0\underline{v} + \sin\phi_0\underline{w}\right]$$

$$\frac{\partial \mathcal{U}_g}{\partial \chi_s} = g\left[\sin\theta_0\underline{N_u}^T + \cos\theta_0\sin\phi_0\underline{N_v}^T + \cos\theta_0\cos\phi_0\underline{N_w}^T\right]$$

Deformations influence the rigid behaviour (Eq. 24) with the term $\cos\phi_0\underline{v}$, and the rigid angles influence the flexible movement by $\sin\theta_0\underline{N_u}^T$.

Let us detail now the aerodynamic forces and analyze how they get into the Lagrange's equations.

2.7 Generalized Aerodynamic Forces

So as to take into account the aerodynamic forces, the Principle of Virtual Work will be used. Therefore, the virtual displacement and the efforts have to be expressed in function of the degrees of freedom chosen before.

The virtual work may be expressed as follows:

$$\delta\mathcal{W} = \boldsymbol{F}\cdot\delta\boldsymbol{r} + \boldsymbol{M}\cdot\delta\boldsymbol{\Omega} \quad (24)$$

where $\boldsymbol{F}$ is the vector of aerodynamic forces projected in the body frame and $\delta\boldsymbol{r} = \delta\boldsymbol{R}^{O_N P}$ is the virtual displacement of the application point P of the forces, $\boldsymbol{M}$ represents the aerodynamic moments projected in the body frame, $\delta\boldsymbol{\Omega}$ the virtual rotation.

The virtual displacement In projection in the body frame F_B, the expression of $\boldsymbol{r} = \boldsymbol{R}^{O_N P}$ is

$$\boldsymbol{r} = \begin{Bmatrix} x_0 \\ y_0 \\ z_0 \end{Bmatrix} + \begin{Bmatrix} p_x \\ p_y \\ p_z \end{Bmatrix} + \begin{Bmatrix} u_P \\ v_P \\ w_P \end{Bmatrix}$$

where the last term is only due to the structural deformations, and is expressed as a function of χ_s; the virtual displacement of P relative to the reference frame F_N is

$$\delta\boldsymbol{r} = \begin{Bmatrix} \delta x_0 \\ \delta y_0 \\ \delta z_0 \end{Bmatrix} + \begin{Bmatrix} \delta u_P \\ \delta v_P \\ \delta w_P \end{Bmatrix} + \{\delta^N\omega^B\} \wedge \begin{Bmatrix} x_0 + s_{x_P} \\ y_0 + s_{y_P} \\ z_0 + s_{z_P} \end{Bmatrix}$$

with $\{\delta^N\omega^B\}^T = \{\,\delta\phi_b\ \delta\theta_b\ \delta\psi_b\,\}$

The virtual rotation $\delta\boldsymbol{\Omega}$ (cf (Eq. 24)) is the local rotation at the point P, relative to the reference frame F_N, and projected in the body frame F_B:

$$\delta\boldsymbol{\Omega} = \begin{Bmatrix} \delta\phi_b + N_{\theta_x}\delta\chi_s \\ \delta\theta_b + N_{\theta_y}\delta\chi_s \\ \delta\psi_b + N_{\theta_z}\delta\chi_s \end{Bmatrix}$$

Generalized aerodynamic forces The efforts on the wing are applied at the aerodynamic center, then, the virtual displacement seen previously will be taken at this point. The quasi-stationnary aerodynamics is modelized with the Lifting Line Theory, and the unstationnary aerodynamics (not yet implemented) with Theodorsen's theory.[8]

Pendaries

Considering the virtual displacement expression, one can obtain the generalized aerodynamic forces:

$$\begin{aligned}\frac{\partial \mathcal{W}}{\partial x_0} &= F_x \\ \frac{\partial \mathcal{W}}{\partial \phi_b} &= F_z y_0 - F_y z_0 + \int s_{y_{ac}} dF_z - \int s_{z_{ac}} dF_y + M_x\end{aligned} \tag{25}$$

$$\begin{aligned}\frac{\partial \mathcal{W}}{\partial \chi_s} = \int \{ & N_u{}^T dF_x + \left(N_w{}^T - d_{Gac} N_{\theta_y}{}^T\right) dF_z \\ & + N_{\theta_x}{}^T dM_x + N_{\theta_y}{}^T dM_y + N_{\theta_z}{}^T dM_z\}\end{aligned} \tag{26}$$

we see now the interest of writing in a new way (Eq. 25) which is simplier:

$$\begin{aligned}\frac{\partial \mathcal{W}}{\partial \phi_b} - y_0 \frac{\partial \mathcal{W}}{\partial z_0} + z_0 \frac{\partial \mathcal{W}}{\partial y_0} = & \int s_{y_{ac}} dF_z \\ & - \int s_{z_{ac}} dF_y + M_x\end{aligned}$$

Aerodynamic efforts dF_x, dF_z are the elementary aerodynamic forces for a surface $c\ dy$ projected in the body frame F_B.

The efforts are often expressed in the aerodynamic frame F_A as we will see later. We will then have to project them in the body frame.

$$\begin{Bmatrix} dF_x \\ dF_y \\ dF_z \end{Bmatrix} = [\mathcal{T}] \begin{Bmatrix} dF_{x_a} \\ dF_{y_a} \\ dF_{z_a} \end{Bmatrix} \tag{27}$$

with

$$[\mathcal{T}] = \begin{bmatrix} -\cos\alpha_{proj}\cos\beta_{loc} & \cos\alpha_{proj}\sin\beta_{loc} & \sin\alpha_{proj} \\ \sin\beta_{loc} & \cos\beta_{loc} & 0 \\ -\sin\alpha_{proj}\cos\beta_{loc} & \sin\alpha_{proj}\sin\beta_{loc} & -\cos\alpha_{proj} \end{bmatrix}$$

where β_{loc} is the local slideslip angle not expressed here, and α_{proj} detailed after.

The elementary drag (for an element of surface $c\ dy$) expressed in the aerodynamic frame is:

$$dF_{x_a} = -\frac{1}{b}\rho S V_a^2 \left(C x_0 + k C z_\alpha^2 \alpha_{loc}^2\right)\ dy$$

the lateral force,

$$dF_{y_a} = \frac{1}{b}\rho S V_a^2 C y_\beta \beta_{loc}\ dy$$

and the lift

$$dF_{z_a} = -\frac{1}{b}\rho S V_a^2 C z_\alpha \alpha_{loc}\ dy$$

Only, the longitudinal terms will be detailed in the following sections.

The elementary pitching moment is given by:

$$dM_y = \frac{1}{b}\rho S c V_a^2 Cm\ dy$$

where

$$Cm = Cm_0 + Cm_\alpha \alpha_{loc} + Cm_q \frac{\left(\dot{q} + \dot{\theta}_y\right) c}{V_a} + Cm_{\delta m}\delta m$$

The aerodynamic velocity and the different angles, α_{loc} and α_{proj} are expressed in the following sections.

Aerodynamic velocity V_a The local aerodynamic velocity at a point P, $V_{aP} = \frac{^N d}{dt}\boldsymbol{R}^{O_N P}$ is given by:

$$V_{aP} = \frac{^N d}{dt}\boldsymbol{R}^{O_N G_0} + \frac{^B d}{dt}\boldsymbol{R}^{G_0 P} + {}^N\boldsymbol{\omega}^B \wedge \boldsymbol{R}^{G_0 P}$$

In the lifting line theory, quantities, like velocity and the angle of attack are referenced with respect to the aerodynamic center. $\frac{^N d}{dt}\boldsymbol{R}^{O_N G_0{}^T} = \{-U\ V\ W\}$ represents the global velocity, the speed of G_0, the origin of the body frame, $\frac{^B d}{dt}\boldsymbol{R}^{G_0 ac} + {}^N\boldsymbol{\omega}^B \wedge \boldsymbol{R}^{G_0 ac}$ is the relative speed of the aerodynamic center and may be expressed as a function of the structural degrees of freedom. In this expression of V_a there are terms of first order in little displacements.

The second term of V_a will introduce a coupling between rigid and flexible due to aerodynamic efforts. The components of V_a projected in the body frame will appear in the angle of attack expression and induce also a strong coupling.

Local angle of attack α_{loc} The local angle of attack is due to several influences Fig. 3, page 7:

- the wedging angle α_c
- the torsion angle θ_y expressed as a function of χ_s
- the angle of attack due to the vertical velocity $\arctan\left(\frac{V_{a_z}}{V_{a_x}}\right)$, expressed as a function of the global velocity and the structural displacements.

Projection angle α_{proj} The aerodynamic efforts are written in the aerodynamic frame and have to be projected in the body frame, so as to be included in the Lagrange's equations (Eq. 25), (Eq. 26).

Considering only the longitudinal flight, so as to simplify, the projection angle α_{proj} has the expression $\arctan\left(\frac{V_{a_z}}{V_{a_x}}\right)$ (cf Fig. 3, page 7).

The main parameters of the local aerodynamic efforts have been expressed in function of the global displacement and the structural displacements. The forces will be integrated along the wing span and participate to the entire aircraft dynamics.

2.8 Conclusion

The Lagrange's equations are now expressed and take into account the full coupling between rigid-body modes and flexible modes. In comparison to the usual approaches,[2,3] the expression of aerodynamic forces

Pendaries

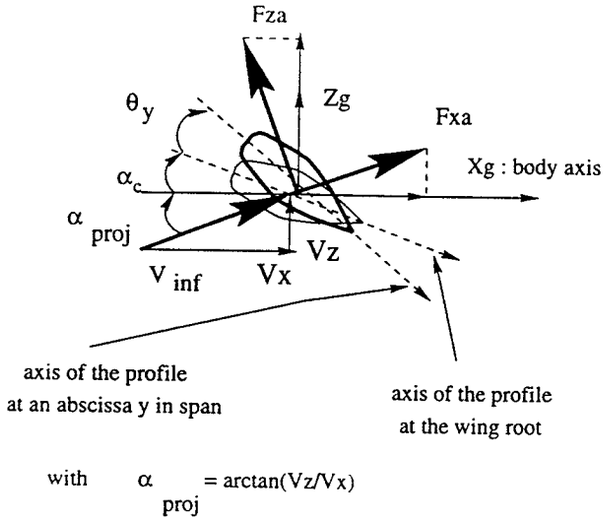

with $\alpha_{proj} = \arctan(Vz/Vx)$

Fig. 3. Projection angle of local aerodynamic efforts

is not more complex. The only supplementary terms of coupling are present in the kinetic energy and reflect a supplementary influence of the rigid on the flexible and the other way round. The system of equations is obviously non linear; the equilibrium point has to be calculated by fixing the global speed and the angle of attack. Around this equilibrium, one can then study the aircraft dynamics through linearization.

The next section is devoted to describe the first results concerning the evolution of rigid and flexible modes in several cases.

3. First Results

3.1 Introduction

The following results represent a kind of validation of the recently implemented program *Super Flutty*, software of simulation of flexible aircraft dynamics.

The aircraft taken as example is the Condor, whose wing characteristics were detailed in[1] and the body is considered as rigid.

Several cases will be presented in the following sections: the first one is the evolution of a flexible aircraft toward an embedded wing to analyze the flutter speed trend; the second case is an evolution from a very rigid wing to a flexible one, to try to have a qualitative idea of this variation; these two cases are calculated for the normal mass and inertia of the Condor.

The last one is the evolution of the kind of instability when the pitching inertia decreases.

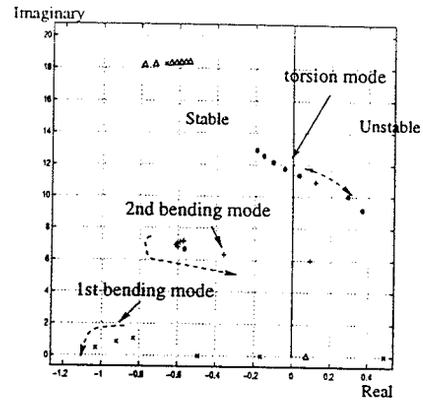

Fig. 4. Evolution of modes (embedded wing)

3.2 From embedded wing to free aircraft ...

This section deals with the influence of rigid-body modes on the flutter speed and on the flexible modes behaviour. It represents a kind of validation of *Super Flutty*. The aim is to try with *Super Flutty* to tend to the case of the embedded wing, computed with *Flutty*, by increasing the body mass and inertia, so as to reduce the influence of rigid-body modes on the flexible modes. In order to balance the increase in mass and to have the same flight cases, a complementary artificial lift had been added at the global center of gravity. Then, the embedded wing should be the limit for very important body mass and inertia. The embedded wing is studied first, then the real free aircraft is presented. The last part shows the results obtained with a body mass of 50 000 kg, instead of 3 950 kg.

The embedded wing The evolution of the flexible modes is plotted on Fig. 4, page 7, thanks to *Flutty*.[1]

Without aerodynamic forces, the frequencies are the following: the first bending mode frequency is about 0.274 Hz, the second bending mode about 1.1982 Hz, and the torsion mode about 2.4803 Hz. The coupling between torsion and bending is stronger than in the previous section, and then the flutter arrives sooner, around 98 m/s. The flutter is here a classical instability of the torsion mode with an energetic exchange with the bending modes. The second bending mode is also on the way of instability. The first bending mode is becoming aperiodic but stable.

The real aircraft The body mass is 3950 kg, its inertia is about 200 000 $kg.m^2$, and the structural coupling between torsion and bending is exactly the same than in the last paragraph, that is to say that center of torsion and center of mass of the profile are exactly in the same position as previously.

The first bending mode frequency is 0.314 Hz and the torsion mode one is 2.486 Hz. The torsion frequency is not affected a lot by the limit conditions.

Pendrais

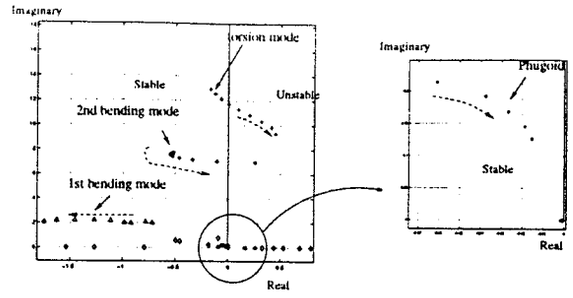

Fig. 5. Evolution of modes (real aircraft)

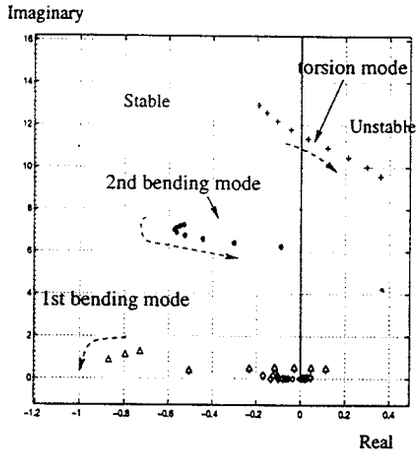

Fig. 6. Evolution of modes (Body mass = 50000 kg)

As you can see on Fig. 5, page 8, the global evolution of the modes are quite equivalent. The instability is a flutter of torsion, but this instability arrives a little bit sooner (around 95 m/s) than in the embedded wing case. Instinctively, I would have said that, in the case of free aircraft and in the same coupling conditions, the flutter should arrive later than for an embedded wing. Nevertheless, the frequencies of the two modes, first bending and torsion modes, are closer than in the previous case. There is a torsion angle at the wing-root, that increases the torsion at the wing tip, and locally increases the aerodynamic forces and thus the coupling between torsion and bending. The rigid-body modes could also contribute to flutter, by a coupling with the flexible modes. This could explain the lower flutter speed, although the difference is not so important.

Note that the first bending mode is no more aperiodic. This is probably the influence of the rigid-body modes. The short period mode, normaly periodic and stable becomes aperiodic very soon, probably because of the flexible modes. The phugoid, like for Fig. 10, page 9, is less and less damped. Its pulsation decreases with speed. This last behaviour is typical of flexible aircraft.

Body-mass = 50 000 kg The modes without aerodynamics are exactly the same than for the embedded wing. The evolution of the modes is also similar to the one in the case of the embedded wing. This shows that when the body mass and inertia are important there is no more coupling between rigid-body modes and flexible modes.

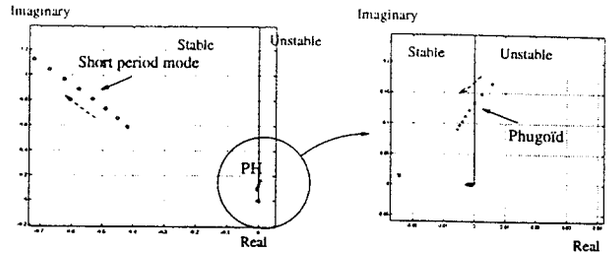

Fig. 7. Evolution of rigid-body modes (rigid aircraft)

Conclusion This section shows that through continuity, the embedded wing flutter is recovered. In this case, the aeroelastic behaviour of the free flexible aircraft is not very different from the one of the embedded wing. This is always torsion instability. But a little difference between the two flutter speeds could be explained by two influences: first of all, the frequencies of the two modes are closer, and the rigid-body modes could contribute to the coupling. Nevertheless, the evolution of the first bending mode is well affected; in the case of free aircraft, it is no more aperiodic.

3.3 From Rigid to Flexible...

This section aims at showing the evolution of the dynamics of the whole flexible aircraft, when the wing is more and more rigid. The longitudinal Young Modulus of the wing had been increased. Then, the coupling between rigid and flexible is changing.

Concerning the body characteristics, its mass is 3950 kg and its pitching inertia is about 200 000 $kg.m^2$. The evolution of the rigid-body modes with the air speed is shown on Fig. 7, page 8. The pulsation of the short-period mode is linear and the damping increases with the speed, and the damping ratio is constant.

Concerning the phugoid, its period is equal to 0.45 . V and the pulsation decreases with the speed, the damping increases.

Note that for low speeds, the phugoid mode is unstable. This is probably due to a coupling between low frequency mode and phugoid, because of an unusual high angle of attack. Indeed, the phugoid computation with the 2 by 2 model (V and γ) gives conventional results in terms of phugoid period and damping, whereas with the complete model (5 by 5) the phugoid is unstable.

Now we will analyze the results, for the same aircraft, but where flexibility had been taken into account. Several Young Modulus for the spar flanges had been considered (500 Mpa, 250 MPa, 140 MPa).

Pendaries

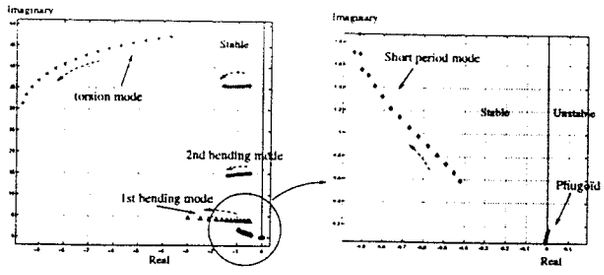

Fig. 8. Evolution of modes (E=500 MPa)

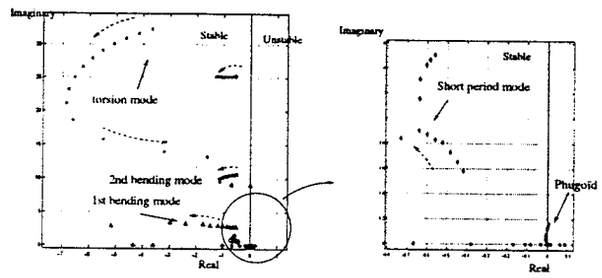

Fig. 9. Evolution of modes (E=250 MPa)

The last value is the Young Modulus of carbon fiber composites with orientation 0^o.

E=500 Mpa On Fig. 8, page 9, the evolution of the rigid and flexible modes with speed is represented. Without aerodynamic efforts, the torsion mode frequency is about 5.2 Hz and the first bending mode frequency about 0.85 Hz. There is no instability on the speed range considered here. The damping of every mode increases and the evolution of the rigid-body modes is not affected by the flexible modes. The phugoid has always the same aspect. Note the apparition of coupling between torsion and bending detected through the decreasing of torsion damping.

E=250 Mpa On Fig. 9, page 9, the coupling between torsion and bending is much stronger than previously, the frequency mode without aerodynamics is about 0.43 Hz for bending and 5.18 Hz for torsion. Since the aerodynamic coefficient Cm_q is very strong and the structural coupling between torsion and bending is not very strong, the second bending mode becomes unstable before the torsion mode. The first bending mode becomes aperiodic, which is characteristic of a very low frequency bending mode.

Concerning the rigid-body mode evolution, the short-period mode is markedly affected, the damping begins to decrease for high speed, and the phugoid mode becomes aperiodic and then unstable.

E=140 Mpa For $E = 140\ Mpa$, the bending frequency is about 0.33 Hz, and the torsion at about 3.69 Hz. The flutter is encountered at a lower speed, and the first bending mode becomes also unstable

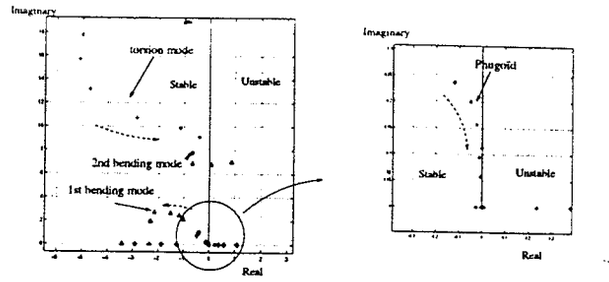

Fig. 10. Evolution of modes (E=140 MPa)

earlier. But what is more interesting, is the evolution of the phugoid mode: the damping is decreasing with speed instead of increasing and the mode is nearly unstable. This is typical for highly flexible systems.[5]

Conclusion This section has shown the influence of flexible modes on the rigid-body modes. By decreasing the wing stiffness, the short-period mode becomes aperiodic, whereas for a rigid aircraft, it was always oscillatory and stable. The phugoid mode has a completely different evolution with the speed when the Young Modulus is decreasing. We have reproduced a typical behaviour of highly flexible aircraft.

3.4 Low Body Mass and Pitching Inertia

This section aims at showing the influence of the body mass and inertia on the flexible modes. Instead of a body mass of 3950 kg, and an inertia of 200 000 $kg.m^2$, the mass is 1000 kg and the inertia 4 000 $kg.m^2$. The short-period mode has then a high frequency compared with the natural aircraft, because ω_{SP} is proportional to $\sqrt{\frac{1}{B}}$ where B is the inertia. The phugoid should not be really affected by this modification.

The rigid behaviour is represented on Fig. 11, page 10. Frequencies and dampings have to be compared with those plotted Fig. 7, page 8, because the same static marge is taken for both examples. For the same air speed, the short-period mode damping and pulsation have a proportionality ratio of $\sqrt{50}$ that is well respected. Concerning the phugoid mode, note that it is no more unstable at low speed with high angle of attack. This is probably due to the fact that the two movements are more decoupled. The terms concerning the short period are bigger because divided by the mass M or the pitching inertia B.

Fig. 11, page 10 will be now compared with Fig. 12, page 10, which represents the evolution of the rigid-body and flexible modes with the speed. The first remark is that there is no more a classical instability, of torsion or of second bending mode, as in the last cases. The torsion damping variates as if there were no coupling. The short period is represented with triangles

Pendcuts

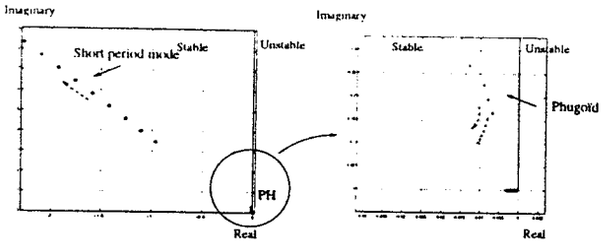

Fig. 11. Evolution of rigid-body modes (Body mass = 1000 kg)

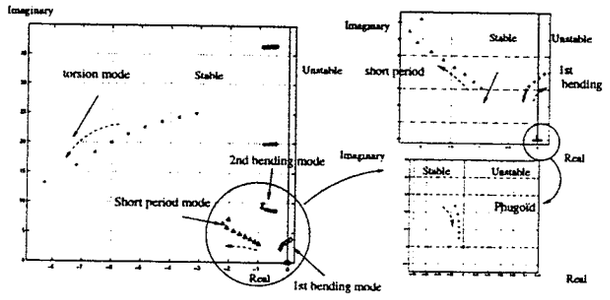

Fig. 12. Evolution of flexible aircraft modes (Body mass = 1000 kg)

and is above the first bending mode (diamonds) in frequency. It has a normal evolution until the speed of 130 m/s, where the damping begins to decrease. Note that the phugoid mode becomes aperiodic probably because of the interaction with flexible modes. Concerning the first bending mode, it has a completely unusual behaviour; the damping decreases with speed instead of increasing and it becomes unstable. This evidences the coupling between short-period and first bending mode. The energetic exchange is between these two modes, and the short period mode plays the role of the torsion. Short period mode gives energy to first bending mode to become unstable. This type of instability is similar to a flapping movement. It is close to flutter conditions of a tailless aircraft with low pitching inertia, the Ricochet.[6,7] For this aircraft, the flutter was an unusual instability of the first bending mode, with a high displacement of the wing root and a very small displacement of the wing tip.

3.5 Conclusion

All these computations show clearly the influence of the coupling between rigid and flexible movements on the evolution of the different modes. The first section was dedicated to the program validation, to follow the evolution of the flexible modes, when the effect of the rigid-body modes was reduced. The action of the flexible modes on the rigid behaviour is shown in the second section, and the last section deals with the influence of the rigid-body modes on the flexible modes.

Two types of instabilities have been detected: the classical flutter with instability of torsion mode by coupling with bending modes; the instability of the first bending mode through the coupling with the short-period mode, creating a kind of flapping movement, as the pitching inertia decreases. The instability of the phugoid, frequently cited in the litterature on flexible aircraft , was not reproduced here; but a tendency to instability had been noticed for the real aircraft.

4. Propulsion by Flapping

The concept of an ornithopter had been presented in the preceeding published article.[1] This concept was thought to answer to design problems; indeed, very especially designed propellers are necessary to be effective at high altitude, where air rarefies. The idea was to take advantage of the wing flexibility, usually seen as a constraint, and by exciting the natural modes in a flapping movement, to produce thrust.

The originality of the concept lies in the fact that we use the natural aircraft, without articulations at the wing root.

In,[1] the theory of flapping is introduced and will not be presented here. In this paper, the flapping of a free wing will be treated, whereas in,[1] the flapping of an embedded wing was studied. We will see here the evolution of the efficiency and the propulsion power due to the flapping of the wing with the inverse of the reduced frequency $(1/k)$, $k = \frac{\omega c}{2V}$.

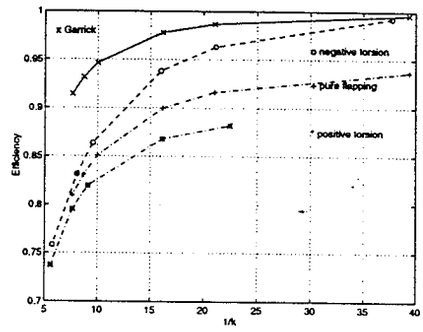

Fig. 13. Evolution of efficiency with 1/k

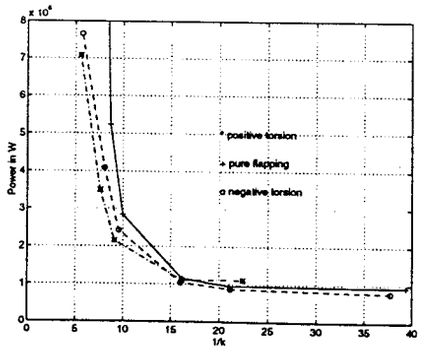

Fig. 14. Evolution of propulsive power with 1/k